

A Novel Red-Emitting Phosphor $\text{Sr}_9\text{Zn}_{1.5}(\text{PO}_4)_7 : \text{Eu}^{3+}$: Synthesis and Photoluminescence Properties^①

LI Jin-feng¹ LI Bao-hui¹ LIU Xue-xia¹ LI Huai-yong¹
HU Cheng-chao¹ ZHENG Bin² SUN Wen-zhi¹

(1. School of Materials Science and Engineering, Liaocheng University, Liaocheng 252059, China; 2. School of Chemistry and Chemical Engineering, Liaocheng University, Liaocheng 252059, China)

Abstract A novel red-emitting phosphor $\text{Sr}_9\text{Zn}_{1.5}(\text{PO}_4)_7 : \text{Eu}^{3+}$ was synthesized by solid-state method. The phase identification and crystal structure were detected by XRD and Rietveld refinement, respectively. The photoluminescence properties were investigated by excitation and emission spectra as well as temperature-dependent luminescence spectra. The phosphor shows strong absorption at 395 nm, matching well with the commercial n-UV chips. Under the excitation of 395 nm, $\text{SZPO} : \text{Eu}^{3+}$ shows bright red emission with the dominate peak at 617 nm, assigning to ${}^5\text{D}_0 \rightarrow {}^7\text{F}_2$ transition of Eu^{3+} . Meanwhile, the fluorescence lifetime and thermal stability of $\text{SZPO} : \text{Eu}^{3+}$ have been investigated in detail. The CIE coordinates of $\text{SZPO} : 0.70\text{Eu}^{3+}$ are (0.616, 0.382). The results indicate $\text{SZPO} : \text{Eu}^{3+}$ may serve as a potential red-emitting phosphor for WLEDs application.

Key words photoluminescence; red emission; phosphor; $\text{SZPO} : \text{Eu}^{3+}$; WLEDs

CLC O644.1

Document code A

0 Introduction

White light-emitting diodes (WLEDs) have drawn wide attention due to their advantages, such as high brightness, long operation time, great stability and low power consumption^[1,2], and they are regarded as the next generation lighting sources^[3]. The popular way to produce WLEDs is to couple blue-emitting InGaN chips with yellow $\text{Y}_3\text{Al}_5\text{O}_{12} : \text{Ce}^{3+}$ phosphor^[4]. Although this is an efficient approach, there exists an obvious shortage according to the tricolor theory. That is, it usually generates cool white light with poor color rendering index (CRI) and relatively high correlated color temperature (CCT) owing to the lack of red component in the spectrum^[5]. To overcome the disadvantages, one method is to couple near ultraviolet (n-UV) chips with RGB (red/green/blue) phosphors to obtain white light with excellent properties. However, the commonly used red phosphors are sulfide-based and nitride-based ones, which suffer some problems. For instance, oxysulfides and sulfides are chemically instable and moisture-sensitive^[6,7]. Furthermore, the commercially available $\text{Y}_2\text{O}_2\text{S} : \text{Eu}^{3+}$ shows low efficiency under n-UV excitation^[8]. Nitrides and oxynitrides are difficult to prepare owing to the demanding synthe-

① 收稿日期:2018-08-31

基金项目:国家自然科学基金项目(51802137, 51701091);聊城大学博士启动基金项目(318051732)资助

通讯作者:孙文芝,女,汉族,博士,讲师,研究方向:发光材料,E-mail:sunwenzhi@lcu.edu.cn.

sis conditions of high temperature and nitrogen pressure^[9]. Hence, it is imperative to explore novel red-emitting oxide-based phosphors excited efficiently by n-UV light.

To find efficient red-emitting phosphors, the choice of activators is a key factor. As is well-known, Eu^{3+} ion has been considered to be an efficient red-emitting activator because of its ${}^5\text{D}_0\text{-}{}^7\text{F}_J$ ($J=0, 1, 2, 3, 4$) transitions, and many Eu^{3+} -doped red-emitting phosphors have been studied^[8,10]. In general, the PLE spectrum of Eu^{3+} consists of charge transfer bands (CTB) in short-wavelength UV region and direct excitation bands in n-UV and blue region.^[11] The excitation bands at n-UV region can match well with the n-UV chips.

As a significant family of luminescent host materials, phosphates have drawn wide attention because of their advantages of easy synthesis, low cost and excellent optical properties^[8]. $\text{Sr}_9\text{Zn}_{1.5}(\text{PO}_4)_7$ is one variation of the whitlockite-type structures that have three P sites (P1-P3) and six metal sites (M1-M6). This special structure enables the rich heterovalent substitution of M^{2+} by quadrivalent (R^{4+}), monovalent (M^+) and trivalent (R^{3+}) cations^[12]. These different replacements of the initial structure can generate many types of materials with whitlockite-type structure, which makes $\text{Sr}_9\text{Zn}_{1.5}(\text{PO}_4)_7$ a feasible host for luminescent materials. In this article, we prepared a novel red-emitting $\text{Sr}_9\text{Zn}_{1.5}(\text{PO}_4)_7:\text{Eu}^{3+}$ phosphor that can be efficiently excited by n-UV light. The powder X-ray diffraction patterns were used to confirm the phase purity. The crystal structure and luminescence properties were studied systematically. Meanwhile, the fluorescence decay curves and thermal quenching properties were also discussed.

1 Experimental Section

1.1 Materials and Synthesis

A series of $\text{Sr}_{9-x}\text{Zn}_{1.5}(\text{PO}_4)_7:x\text{Eu}^{3+}$ (SZPO: $x\text{Eu}^{3+}$) ($x=0-0.90$) and $\text{Sr}_{7.8}\text{Zn}_{1.5}(\text{PO}_4)_7:0.60\text{Eu}^{3+}$, 0.60M^+ ($\text{M}^+=\text{Li}^+$, Na^+ and K^+) phosphors were synthesized by solid-state method. The starting materials SrCO_3 (A. R.), ZnO (A. R.), $\text{NH}_4\text{H}_2\text{PO}_4$ (A. R.) and Eu_2O_3 (99.99%) were weighed in stoichiometric ratio. The mixtures were ground thoroughly in the agate mortar, and firstly sintered at 450°C for 3 h with the heating rate of $3^\circ\text{C}/\text{min}$. Then, the reground powders were calcined at 1250°C for 6 h with the heating rate of $3^\circ\text{C}/\text{min}$ in air. Eventually, as-obtained samples were ground into powder for further measurements.

1.2 Materials Characterization

The powder X-ray diffraction (XRD) data were collected by a D8 Focus diffractometer operating at 40 kV and 40 mA with graphite-monochromated $\text{Cu K}\alpha$ radiation ($\lambda=0.15405\text{ nm}$). Rietveld refinements of the XRD data were performed with the software GSAS. The excitation and emission spectra were detected on a Hitachi F-7000 spectrophotometer with the excitation source of a 150 W xenon lamp. The fluorescence decay curves were collected from a Lecroy Wave Runner 6100 Digital Oscilloscope (1 GHz) with a tunable laser (pulse width=4 ns, gate=50 ns) as the excitation source. The temperature-dependent PL spectra were detected on a Maya 2000 spectrophotometer (Ocean Optics) with a heating apparatus.

2 Results and Discussion

2.1 Phase Purity and Crystal Structure

Fig. 1(a) shows the XRD profiles together with the standard data $\text{Sr}_9\text{Fe}_{1.5}(\text{PO}_4)_7$ (JCPDS card No. 51-0427). As $\text{Sr}_9\text{Mg}_{1.5}(\text{PO}_4)_7$ is isostructural with $\text{Sr}_9\text{Fe}_{1.5}(\text{PO}_4)_7$ ^[13], from Fig. 1(a), one can obviously find that all XRD patterns of $\text{SZPO}:x\text{Eu}^{3+}$ agree well with the standard data $\text{Sr}_9\text{Fe}_{1.5}(\text{PO}_4)_7$, which manifests that the doped Eu^{3+} ions do not generate any notable impurities. As for the site occupancy, considering the similar ionic radii of Eu^{3+} (1.066 \AA , CN=8) and Sr^{2+} (1.26 \AA , CN=8)^[14], we suppose that Eu^{3+} ions are tend to occupy the Sr^{2+} sites. What's more, it is also obvious from Fig. 1(a) that the positions of the diffraction peaks shift gradually to larger 2θ degree with the Eu^{3+} concentration x in-

creasing from 0 to 0.9, because of the cell shrink of $\text{Sr}_9\text{Mg}_{1.5}(\text{PO}_4)_7$ host resulting from Eu^{3+} with small ionic radius substituting for Sr^{2+} with large ionic radius.

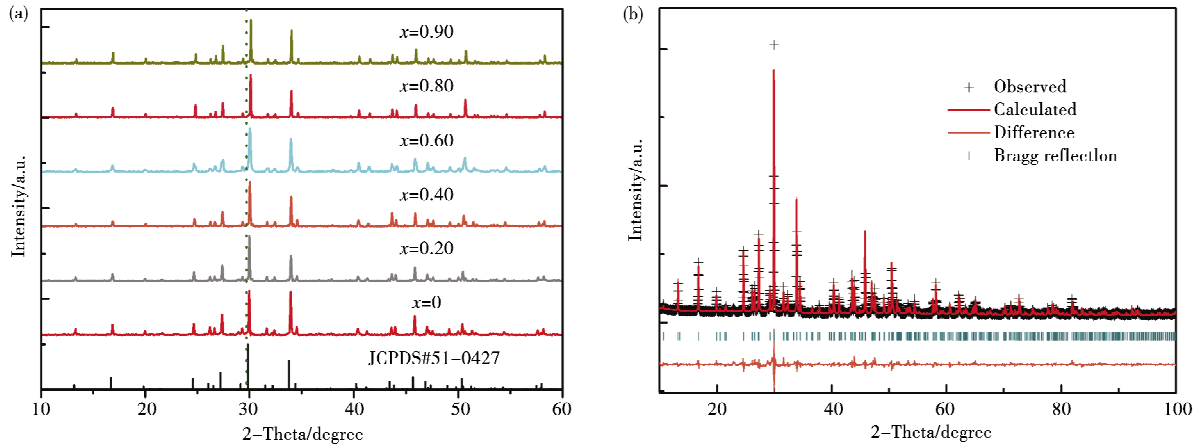


Fig. 1 (a) The XRD profiles of SZPO: $x\text{Eu}^{3+}$ ($x=0, 0.20, 0.40, 0.60, 0.80$ and 0.90) and the standard data $\text{Sr}_9\text{Fe}_{1.5}(\text{PO}_4)_7$ (JCPDS card No. 51-0427); (b) The Rietveld refinement pattern of SZPO: 0.50Eu^{3+}

Fig. 1 (b) shows the Rietveld refinement patterns of SZPO: 0.50Eu^{3+} . Table 1 lists the refinement results and the structure data of SZPO: 0.50Eu^{3+} . The refinements finally converged to $\chi^2 = 3.507$, $R_p = 4.80\%$, $R_{wp} = 6.51\%$, which indicates that the atom positions, fraction factors and temperature factors of the sample agree well with the reflection conditions. SZPO: Eu^{3+} has the trigonal unit cell with $R\bar{3}m$ as the space group. The cell parameters are $a=b=10.588 \text{ \AA}$, $c=19.693 \text{ \AA}$ and $V=1911.987 \text{ \AA}^3$. Fig. 2 shows the unit structure of $\text{Sr}_9\text{Zn}_{1.5}(\text{PO}_4)_7$. There are three Sr sites (Sr1, Sr31 and Sr32), two Mg sites (Mg4 and Mg5) and two P sites (P1 and P2) in the $\text{Sr}_9\text{Zn}_{1.5}(\text{PO}_4)_7$ matrix^[15]. The structure is highly disordered. The coordination numbers (CN) of Sr1 site is 8, while those of Sr31 and Sr32 sites change with the orientation of PO_4 tetrahedra; 8 or 9 for Sr31 site, and 6 or 7 for Sr32 site.

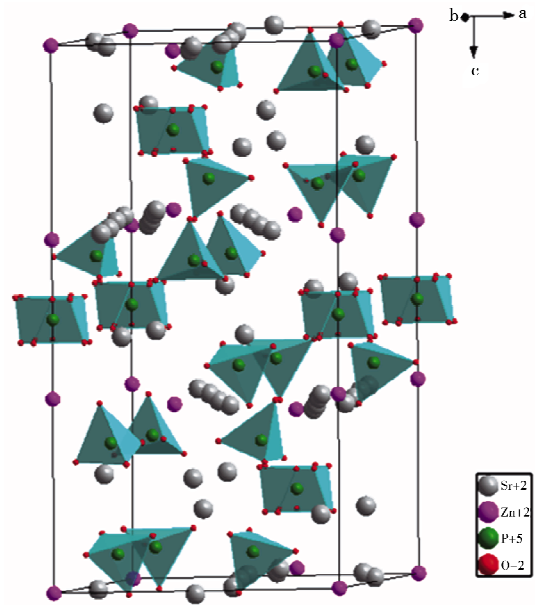


Fig. 2 The unit structure of $\text{Sr}_9\text{Zn}_{1.5}(\text{PO}_4)_7$

Table 1 Rietveld refinement and crystal structure data of $\text{Sr}_{8.5}\text{Zn}_{1.5}(\text{PO}_4)_7: 0.50\text{Eu}^{3+}$

Formula	$\text{Sr}_{8.5}\text{Zn}_{1.5}(\text{PO}_4)_7: 0.50\text{Eu}^{3+}$
Space group	$R\bar{3}m$ (No. 166)
$a=b(\text{ \AA})$	10.588
$c(\text{ \AA})$	19.693
$a=\beta$ (deg)	90
γ (deg)	120
N	3
V (\AA^3)	1911.987
R_p (%)	4.80
R_{wp} (%)	6.51
χ^2	3.507

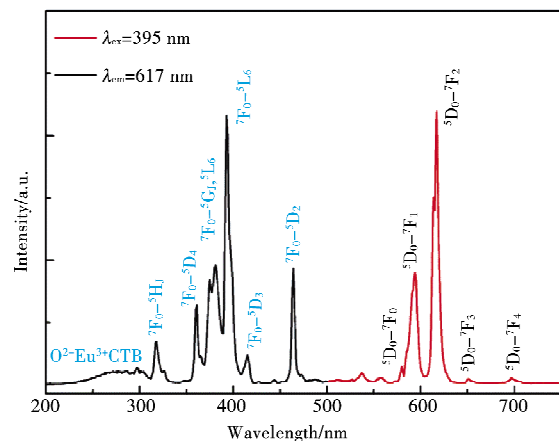


Fig. 3 The PLE and PL spectra of SZPO: Eu^{3+}

2.2 Photoluminescence Properties of SZPO: Eu^{3+}

Fig. 3 shows the PLE and PL spectra of SZPO: Eu^{3+} . Monitored at 617 nm, the PLE spectrum exhibits several sharp peaks and a broad band ranging from 200-310 nm, which is attributed to the charge transfer band of $\text{O}^{2-}-\text{Eu}^{3+}$. The peaks at 317 nm, 360 nm, 380 nm, 395 nm, 415 nm and 465 nm are ascribed to the ${}^7\text{F}_0-{}^5\text{H}_1$, ${}^7\text{F}_0-{}^5\text{D}_4$, ${}^7\text{F}_0-{}^5\text{G}_1$, ${}^5\text{L}_7$, ${}^7\text{F}_0-{}^5\text{L}_6$, ${}^7\text{F}_0-{}^5\text{D}_3$ and ${}^7\text{F}_0-{}^5\text{D}_2$ transitions of Eu^{3+} , respectively. Therein, the 395 nm peak is predominated, and it is consistent with the n-UV commercial chips perfectly, which proves that SZPO: Eu^{3+} may serve as a potential red-emitting phosphor for WLEDs application.

The PL spectrum consists of a series of sharp lines corresponding to the characteristic transitions from the excited state ${}^5\text{D}_0$ to the ground state ${}^7\text{F}_j$ ($J=0, 1, 2, 3, 4$) of Eu^{3+} ions. The strongest peak at 617 nm is ascribed to ${}^5\text{D}_0-{}^7\text{F}_2$ transition and the peak at 594 nm is due to the ${}^5\text{D}_0-{}^7\text{F}_1$ transition. According to the selection rule, the emission peaks belonging to ${}^5\text{D}_0-{}^7\text{F}_1$ and ${}^5\text{D}_0-{}^7\text{F}_2$ transitions are assigned to magnetic dipole transition and electric dipole transition, respectively.^[16] The transition ${}^5\text{D}_0-{}^7\text{F}_2$ is hypersensitive to the environment of the crystal field, while the transition ${}^5\text{D}_0-{}^7\text{F}_1$ is insensitive^[11]. The electric dipole transition ${}^5\text{D}_0-{}^7\text{F}_2$ will predominate in the PL spectra when Eu^{3+} ions occupy a site without inversion symmetry, and conversely, magnetic dipole transition ${}^5\text{D}_0-{}^7\text{F}_1$ will become strongest when Eu^{3+} ions are in an inversion symmetry site. Hence, the emission intensity ratio of $({}^5\text{D}_0-{}^7\text{F}_2)/({}^5\text{D}_0-{}^7\text{F}_1)$ is a good way to explore the site symmetry around Eu^{3+} ions. For SZPO: Eu^{3+} , the emission intensity from electric dipole transition ${}^5\text{D}_0-{}^7\text{F}_2$ is much larger than that from ${}^5\text{D}_0-{}^7\text{F}_1$, indicating that the local symmetry around Eu^{3+} in SZPO: Eu^{3+} is non-centrosymmetric^[2].

Fig. 4(a) shows the PL spectra of SZPO: $x\text{Eu}^{3+}$ with various Eu^{3+} concentrations under the 395 nm excitation. Fig. 4(b) depicts the PL intensities as a function of Eu^{3+} concentration. The PL intensity ascends with the rising of Eu^{3+} concentrations up to $x=0.70$, and then declines beyond that concentrations, which is ascribed to the concentration quenching behavior. The critical distance R_c between Eu^{3+} in SZPO: Eu^{3+} can be obtained according to the following equation^[17]

$$R_c \approx 2 \left[\frac{3V}{4\pi x_c N} \right]^{1/3}, \quad (1)$$

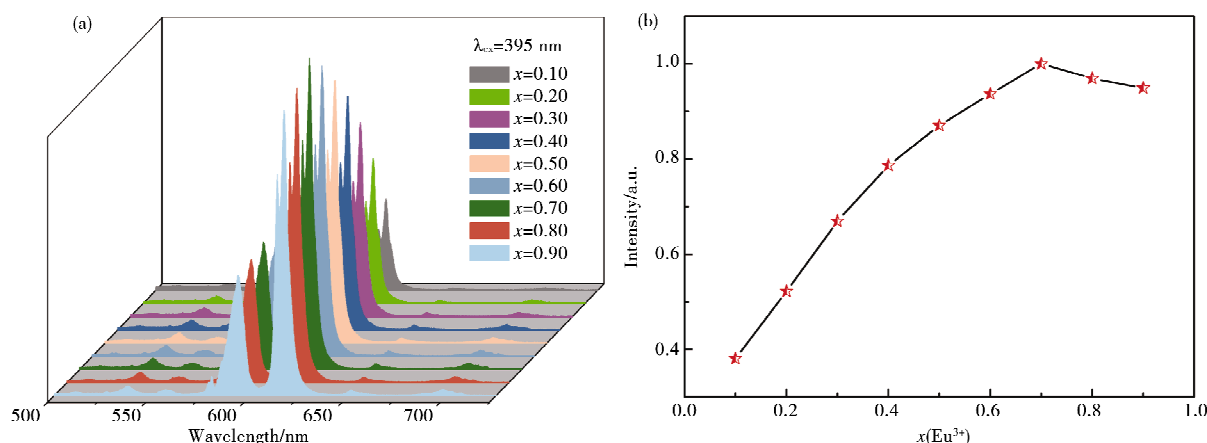


Fig. 4 (a) PL spectra of SZPO: $x\text{Eu}^{3+}$ with various Eu^{3+} concentrations ($\lambda_{ex} = 395 \text{ nm}$);
(b) PL intensities as a function of Eu^{3+} concentration (x)

Where N is the formula units number per unit cell, V is the unit cell volume, and x_c is the obtained critical concentration. With respect to SZPO: $x\text{Eu}^{3+}$, $V=1911.987 \text{ \AA}^3$, $x_c=0.70$ and $N=3$. Therefore, R_c is calculated to be 12.03 \AA . The Commission International de l'Éclairage (CIE) chromaticity coordinates of SZPO: 0.70Eu^{3+} are $(0.616, 0.382)$, which is shown in Fig. 5.

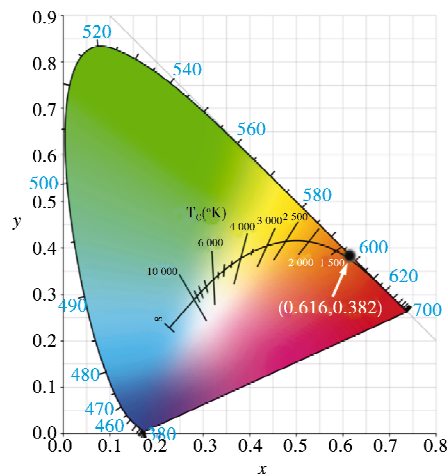


Fig. 5 CIE chromaticity diagram of SZPO: 0.60Eu³⁺ phosphor ($\lambda_{exc}=395$ nm)

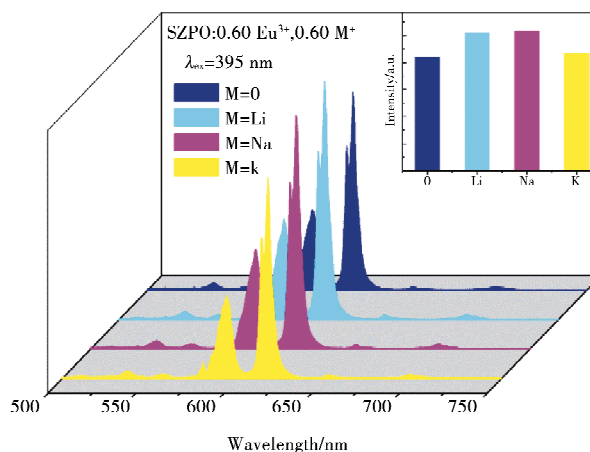


Fig. 6 PL spectra for SZPO: 0.60Eu³⁺, 0.60M⁺ (M⁺ = Li⁺, Na⁺ and K⁺), the inset shows the corresponding integrated PL intensities

Fig. 6 shows the charge compensation effect of different charge compensators (Li⁺, Na⁺ and K⁺) on the PL intensity of SZPO: 0.60Eu³⁺. It can be found that the three charge compensators all can increase the PL intensity of SZPO: 0.60Eu³⁺. And among them, the effect of Li⁺ and Na⁺ is much better than that of K⁺. It may be because the radii of Li⁺ and Na⁺ are a little smaller than that of Sr²⁺, and this make them occupy the Sr²⁺ sites more easily than K⁺, the radius of which is much larger than that of Sr²⁺.

2.3 Fluorescence decay of SZPO: Eu³⁺

Fig. 7 shows decay curves of SZPO: x Eu³⁺ ($x=0.40, 0.50, 0.70$ and 0.90) excited at 395 nm and monitored at 617 nm. The decay profiles can be fitted by single-exponential function^[18]

$$I = A \exp(-t/\tau), \quad (2)$$

Where A is a constant, $I(t)$ is the PL intensity at time t , τ is the decay time of the exponential function, respectively. The average lifetime (τ) can be determined to be 1.92, 1.95, 1.93, and 1.91 ms for SZPO: x Eu³⁺ phosphors with $x=0.40, 0.50, 0.70$, and 0.90 , respectively. The results indicate that the lifetimes for SZPO: Eu³⁺ is in the order of milliseconds, which is in accordance with the most frequent value of the Eu³⁺ emission in solids.

2.4 Thermal Stability of SZPO: Eu³⁺

Fig. 8(a) shows the temperature-dependent PL spectra of SZPO: 0.70Eu³⁺. The PL intensity of SZPO: 0.70Eu³⁺ decreases gradually with temperature increasing from 299 K to 523 K, due to the thermal quenching effect. The emission intensities at 373 K, 498 K and 523 K only decline to 88.5%, 64.7% and 55.0% of the initial one, respectively, as shown in the inset of Fig. 8(a). And according to the literature^[19], the emission intensities of the commercial red-emitting phosphor Y₂O₃: Eu³⁺ at 373 K and 508 K decline to about 85% and 54% of the initial one, respectively. The thermal stability of SZPO: Eu³⁺ is similar to that of Y₂O₃: Eu³⁺, which demonstrates that the thermal stability of SZPO: Eu³⁺ is excellent. A modified Arrhenius equation is applied to obtain the activation energy (ΔE) for thermal quenching^[20]

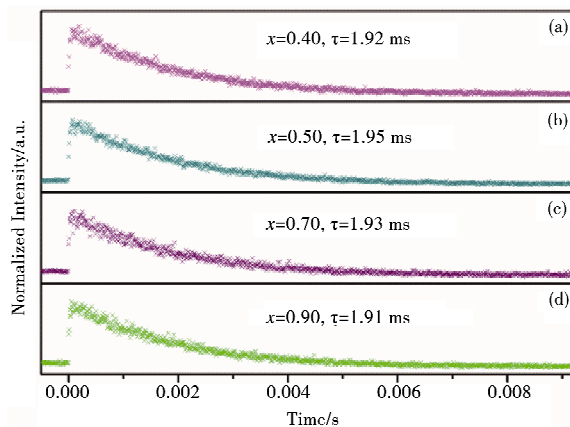


Fig. 7 Fluorescence decay curves of SZPO: x Eu³⁺ ($x=0.40, 0.50, 0.70$ and 0.90) excited at 395 nm and monitored at 617 nm

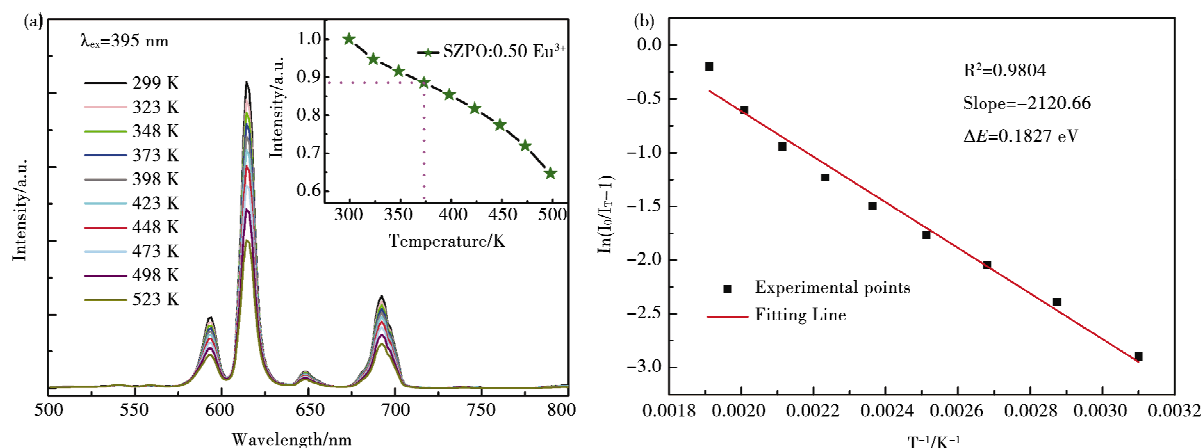


Fig. 8 (a) Temperature-dependent PL spectra of $\text{SZPO}: 0.70\text{Eu}^{3+}$ ($T=299\text{--}523\text{ K}$, $\lambda_{\text{ex}}=395\text{ nm}$); the inset shows the PL intensity of $\text{SZPO}: 0.50\text{Eu}^{3+}$ as a function of temperature (T); (b) The dependence of $\ln[(I_0/I_T)-1]$ on $1/T$ for $\text{SZPO}: 0.70\text{Eu}^{3+}$

$$I_T = \frac{I_0}{1 + c \exp(-\frac{\Delta E}{kT})}, \quad (3)$$

Where I_0 and I_T are the emission intensities at room temperature and experimental temperature, respectively; c is a constant and represents the rate of thermally activated escape; k is the Boltzmann constant ($k=8.617 \times 10^{-5}\text{ eV/K}$); T is the temperature. Based on eq. (3), the relationship of $\ln[(I_0/I_T)-1]$ with $1/T$ is linear with the slope of $-\Delta E/k$. Fig. 8(b) plots the dependence of $\ln[(I_0/I_T)-1]$ on $1/T$ for $\text{SZPO}:0.70\text{Eu}^{3+}$. And the activation energy ΔE was calculated to be 0.1827 eV . The result reveals that $\text{SZPO}: \text{Eu}^{3+}$ can serve as a potential red-emitting phosphor in n-UV WLEDs.

3 Conclusions

A novel red-emitting $\text{Sr}_9\text{Zn}_{1.5}(\text{PO}_4)_7:\text{Eu}^{3+}$ phosphor was synthesized by solid-state reaction. The phosphor can be excited efficiently by n-UV light, and exhibit bright red emission with the dominate peak at 617 nm , assigning to ${}^5\text{D}_0\text{--}{}^7\text{F}_2$ transition of Eu^{3+} . The space group of $\text{SZPO}: \text{Eu}^{3+}$ is $R\bar{3}m$, and the cell parameters are $a=b=10.588\text{ \AA}$, $c=19.693\text{ \AA}$ and $V=1\,911.987\text{ \AA}^3$. The critical distance (R_c) is calculated to be 12.03 \AA . The thermal stability of $\text{SZPO}: \text{Eu}^{3+}$ is similar to that of $\text{Y}_2\text{O}_3:\text{Eu}^{3+}$, which demonstrates that the thermal stability of $\text{SZPO}: \text{Eu}^{3+}$ is excellent. The CIE coordinates of $\text{SZPO}: 0.70\text{Eu}^{3+}$ are $(0.616, 0.382)$. The results demonstrate $\text{SZPO}: \text{Eu}^{3+}$ may serve as a potential red-emitting phosphor for WLEDs application.

References

- [1] Xie R J, Hirosaki N, Mitomo M, et al. Wavelength-tunable and thermally stable Li- α -sialon: Eu^{2+} oxynitride phosphors for white light-emitting diodes[J]. Appl Phys Lett, 2006, 89(24): 241103.
- [2] Zhong J, Chen D, Zhao W, et al. Garnet-based $\text{Li}_6\text{CaLa}_2\text{Sb}_2\text{O}_{12}:\text{Eu}^{3+}$ red phosphors: a potential color-converting material for warm white light-emitting diodes[J]. J Mater Chem C, 2015, 3(17): 4500-4510.
- [3] Bachmann V, Ronda C, Meijerink A. Temperature Quenching of Yellow Ce^{3+} Luminescence in YAG: Ce[J]. Chem Mater, 2009, 21(10): 2077-2084.
- [4] Nakamura S, Fasol G. The Blue Laser Diode: GaN-Based Light Emitting Diode and Lasers[M]. Berlin, Springer, 1997.
- [5] Jia Y, Pang R, Li H, et al. Single-phased white-light-emitting $\text{Ca}_4(\text{PO}_4)_2\text{O}:\text{Ce}^{3+}, \text{Eu}^{2+}$ phosphors based on energy transfer[J]. Dalton Trans, 2015, 44(25): 11399-11407.
- [6] Duan C J, Delsing A C A, Hintzen H T. Photoluminescence Properties of Novel Red-Emitting Mn^{2+} -Activated MZnOS ($M=\text{Ca}, \text{Ba}$) Phosphors[J]. Chem Mater, 2009, 21(6): 1010-1016.
- [7] Li H, Zhao R, Jia Y, et al. $\text{Sr}_1.7\text{Zn}_{0.3}\text{CeO}_4:\text{Eu}^{3+}$ Novel Red-Emitting Phosphors: Synthesis and Photoluminescence Properties[J]. ACS Appl Mater Interfaces, 2014, 6(5): 3163-3169.

- [8] Dong X, Zhang J, Zhang X, et al. New orange-red phosphor $\text{Sr}_3\text{Sc}(\text{PO}_4)_7: \text{Eu}^{3+}$ for NUV-LEDs application[J]. *J Alloys Compd*, 2014, 587: 493-496.
- [9] Hecht C, Stadler F, Schmidt P J, et al. $\text{SrAlSi}_4\text{N}_7: \text{Eu}^{2+}$ -A Nitridoalumosilicate Phosphor for Warm White Light (pc)LEDs with Edge-Sharing Tetrahedra[J]. *Chem Mater*, 2009, 21(8): 1595-1601.
- [10] Wang Z, Lou S, Li P. Luminescent properties and energy transfer of $\text{Sr}_3\text{La}(\text{PO}_4)_3: \text{Sm}^{3+}, \text{Eu}^{3+}$ for white LEDs[J]. *J Alloys Compd*, 2014, 586: 536-541.
- [11] Kang D, Yoo H S, Jung S H, et al. Synthesis and Photoluminescence Properties of a Novel Red-Emitting $\text{Na}_2\text{Y}_2\text{Ti}_3\text{O}_{10}: \text{Eu}^{3+}, \text{Sm}^{3+}$ Phosphor for White-Light-Emitting Diodes[J]. *J Phys Chem C*, 2011, 115(49): 24334-24340.
- [12] Belik A A, Izumi F, Ikeda T, et al. Whitlockite-Related Phosphates $\text{Sr}_3\text{A}(\text{PO}_4)_7$ (A = Sc, Cr, Fe, Ga, and In): Structure Refinement of $\text{Sr}_3\text{In}(\text{PO}_4)_7$ with Synchrotron X-Ray Powder Diffraction Data[J]. *J Solid State Chem*, 2002, 168(1): 237-244.
- [13] Sun W, Jia Y, Pang R, et al. $\text{Sr}_3\text{Mg}_{1.5}(\text{PO}_4)_7: \text{Eu}^{2+}$: A Novel Broadband Orange-Yellow-Emitting Phosphor for Blue Light-Excited Warm White LEDs[J]. *ACS Appl Mater Interfaces*, 2015, 7(45): 25219-25226.
- [14] Shannon R. Revised effective ionic radii and systematic studies of interatomic distances in halides and chalcogenides[J]. *Acta Crystallogr, Sect A*, 1976, 32(5): 751-767.
- [15] Belik A A, Lazoryak B I, Pokholok K V, et al. Synthesis and Characterization of New Strontium Iron(II) Phosphates, $\text{SrFe}_2(\text{PO}_4)_2$ and $\text{Sr}_3\text{Fe}_{1.5}(\text{PO}_4)_7$ [J]. *J Solid State Chem*, 2001, 162(1): 113-121.
- [16] Liu W R, Lin C C, Chiu Y C, et al. $\text{ZnB}_2\text{O}_4: \text{Bi}^{3+}, \text{Eu}^{3+}$: a highly efficient, red-emitting phosphor[J]. *Opt Express*, 2010, 18(3): 2946-2951.
- [17] Blasse G. Energy transfer in oxidic phosphors[J]. *Philips Res Rep*, 1969, 24(2): 131-144.
- [18] Dexter D, Schulman J H. Theory of concentration quenching in inorganic phosphors[J]. *J Chem Phys*, 1954, 22(6): 1063-1070.
- [19] Zhu G, Ci Z, Shi Y, et al. Synthesis, crystal structure and luminescence characteristics of a novel red phosphor $\text{Ca}_{19}\text{Mg}_2(\text{PO}_4)_{14}: \text{Eu}^{3+}$ for light emitting diodes and field emission displays[J]. *J Mater Chem C*, 2013, 1(37): 5960-5969.
- [20] Xu C, Li Y, Huang Y, et al. Luminescence characteristics and site-occupancy of Eu^{2+} and Eu^{3+} -doped $\text{MgZn}_2(\text{PO}_4)_2$ phosphors[J]. *J Mater Chem*, 2012, 22(12): 5419-5426.

红色荧光粉 $\text{Sr}_9\text{Zn}_{1.5}(\text{PO}_4)_7: \text{Eu}^{3+}$ 的制备及发光性质研究

李金锋¹ 李宝慧¹ 刘学霞¹ 李怀勇¹ 胡成超¹ 郑彬² 孙文芝¹

(1.聊城大学 材料科学与工程学院,山东 聊城 252059; 2.聊城大学 化学与化工学院,山东 聊城 252059)

摘要 采用高温固相法合成了一系列近紫外激发的白光 LED 用红色荧光材料 $\text{Sr}_9\text{Zn}_{1.5}(\text{PO}_4)_7: x\text{Eu}^{3+}$. 通过 X 射线粉末衍射和 Rietveld 结构精修分别确定了材料的相纯度和晶体结构. 通过激发光谱和发射光谱研究了材料的发光性质. 该荧光粉可以被 395 nm 近紫外光有效激发,这与商品近紫外芯片的发射光谱吻合. 在近紫外光激发下,样品可以发射出明亮的红光,其最大发射峰在 617 nm,归属于 Eu^{3+} 的 $^5\text{D}_0 \rightarrow ^7\text{F}_2$ 跃迁. SZPO: 0.70 Eu^{3+} 的色坐标为 (0.616, 0.382). 此外,还对材料的荧光衰减和热稳定性进行了系统研究. 实验结果表明, $\text{Sr}_9\text{Zn}_{1.5}(\text{PO}_4)_7: \text{Eu}^{3+}$ 可以作为潜在的白光 LED 用红光荧光粉.

关键词 荧光; 红光; 荧光材料; SZPO: Eu^{3+} ; 白光 LED

中图分类号 O644.1

文献标识码 A